HHS Public Access

Author manuscript

Bone. Author manuscript; available in PMC 2021 August 01.

Published in final edited form as:

Bone. 2020 August ; 137: 115438. doi:10.1016/j.bone.2020.115438.

The BALB/c Mouse as a Preclinical Model of the Age-Related Deterioration in the Lumbar Vertebra

Dominique HarrisS[1], **Kate Garrett, BS**[2], **Sasidhar Uppuganti, MS**[2,3], **Amy Creecy, PhD**[2,3,4], **Jeffry S. Nyman, PhD**[2,3,4,5,*]

[1]Meharry Medical College, 1005 Dr. DB Todd Jr. Blvd. Nashville, TN 37208, USA

[2]Department of Orthopaedic Surgery, Vanderbilt University Medical Center, 1215 21st Ave. S., Suite 4200, Nashville, TN 37232, USA

[3]Center for Bone Biology, Vanderbilt University Medical Center, Nashville, TN 37232, USA

[4]Department of Biomedical Engineering, Vanderbilt University, 5824 Stevenson Center, Nashville, TN 37232, USA

[5]Department of Veterans Affairs, Tennessee Valley Healthcare System, 1310 24th Ave. S., Nashville, TN 37212, USA

Abstract

The likelihood of experiencing an osteoporotic fracture of one or more vertebral bodies increases with age, and this increase is not solely due to sex steroid deficiency. For the purpose of assessing the effectiveness of novel therapeutic strategies in the prevention of vertebral fractures among the elderly, we hypothesized that the BALB/c mouse model of aging phenocopies the age-related decrease in human VB strength. To test this hypothesis, we assessed the age-related changes in trabecular architecture of the L6 VB, with respect to those in the distal femur metaphysis, between 6-mo. (young adulthood, n=20/sex) and 20-mo. of age (old age, n=18/sex) and then determined how well the architectural characteristics, volumetric bone mineral density (vBMD), and predicted failure force from μCT-derived finite element analysis (μFEA) with linear elastic failure criteria explained the age-related variance in VB strength, which was the ultimate force during *quasi*-static loading of the VB in compression. While there was a pronounced age-related deterioration in

[*]**Correspondence:** Jeffry S. Nyman, Vanderbilt Orthopaedic Institute, Medical Center East, South Tower, Suite 4200, Nashville, TN 37232, jeffry.s.nyman@vumc.org, o: (615) 936-6296.

Credit author statement

Dominique Harris: Investigation, Formal analysis, Visualization, Writing Original draft preparation, Writing - Review & Editing.

Kate Garrett: Data curation, Investigation, Formal analysis, Visualization, Writing Original draft preparation, Writing - Review & Editing.

Sasidhar Uppuganti: Investigation, Resources, Data curation, Software, Visualization, Validation, Writing - Review & Editing, Project administration

Amy Creecy: Conceptualization, Methodology, Resources, Validation, Investigation, Writing - Review & Editing

Jeffry S. Nyman: Conceptualization, Methodology, Validation, Formal analysis, Data Curation, Writing Original draft preparation, Writing - Review & Editing, Supervision, Project administration, Funding acquisition

Declaration of competing interests

There authors do not have conflicts of interest to declare.

trabecular architecture in the distal femur metaphysis of female and male BALB/c mice, the decrease in trabecular bone volume fraction and trabecular number between 6-mo. and 20-mo. of age occurred in male mice, but not in female mice. As such, the VB strength was lower with age in males only. Nonetheless, BV/TV and volumetric bone mineral density (vBMD) positively correlated with the ultimate compressive force of the L6 VB for both females and males. Whether using a fixed homogeneous distribution of tissue modulus (E_t = 18 GPa) or a heterogeneous distribution of E_t based on a positive relationship with TMD, the predicted failure force of the VB was not independent of age, thereby suggesting linear μFEA may not be a suitable replacement for mechanical-based measurements of strength with respect to age-related changes. Overall, the BALB/c mouse model of aging mimics the age-related in decline in human VB strength when comparing 6-mo. and 20-mo. old male mice. The decrease in VB strength in female mice may occur over a different age range.

Keywords

osteoporosis; aging; vertebral body strength; preclinical model; trabecular architecture; finite element analysis

1. Introduction

A minimally traumatic fracture of a vertebral body (VB) is one of the more common manifestation of osteoporosis [1,2]. Such fractures involving the spine are the result of low-energy, minor events like driving over speed bumps or falling from standing height. Elderly individuals also present with compression fractures of the VB without recalling any traumatic event [3]. Objective observations on clinical examination may include stooped stature (kyphosis), loss of spinal column height, reduced respiratory expansion, lumbar radiculopathy secondary to intervertebral foramina narrowing, numbness, tingling, or weakness in lower extremities. Using NHANES data from 2005 to 2010, the prevalence of osteoporosis among the US population was estimated to be 8.0% for those between 60 and 69 years of age (women/men = 12.3%/3.3% = 3.7) and 26.2% for those 80 years and older (women/men = 34.9%/10.9% = 3.2) [4]. Irrespective of the higher fracture risk among females, osteoporosis is a problem of aging. Although effective therapies exist to treat osteoporosis, VB fractures remain a major clinical problem because of concerns about long-term side effects, difficulties in diagnosing the disease, and insufficient understanding of the causes of low-energy, fragility fractures of VBs. To prevent the ensuing pain, loss of mobility, and the increased likelihood of another osteoporotic fracture that VB fractures cause, a preclinical model of aging is needed that phenocopies the loss in human VB strength with age.

Ovariectomy (OVX) to model the effects of menopause on bone causes a decrease in bone mass and vertebral body (VB) strength in mice and rats [5,6]. Yet there are other age-related changes - independent of bone mass or bone mineral density (BMD) - that likely lower the fracture resistance of the vertebra in mice [7] and in humans [8]. As such, a new therapeutic strategy ideally would not only reverse or prevent bone loss caused by estrogen deficiency but also combat the deterioration in trabecular architecture and strength that occurs with

aging in human VBs [9–11]. With respect to preclinical models of aging, the National Institute on Aging (NIA) in the US supports several colonies of rodents in which young and old animals are available to investigators through a commercial vendor. Among the multiple rodent strains used in preclinical studies, the age-related decrease in trabecular bone volume fraction (BV/TV) or in areal BMD (aBMD) of lumbar vertebrae has been established for male Fischer F344 rats [12], male Sprague-Dawley rats [13], female CW-1 mice [14], male and female C57BL/6J mice [15–17], sham and OVX C57BL/6J mice [7], and female and male BALB/c mice [18]. On the other hand, the age-related decrease in the compressive strength of the rodent VB is less clear with a significant difference and a lack of difference between young and old animals reported in the literature (Table 1).

Even when the compressive strength of the lumbar vertebra at the whole-bone level was observed to decrease with age for a given rodent strain, the potential cause of the decrease is often not established. For example, in the study of age-related changes in the bones of BALB/c mice [18], the ultimate force of the L5 VB was lower at 20-mo. than at 7-mo. (males) or at 12-mo. (females), but the BV/TV within the centrum was not significantly different between these same 2 age groups in males. Also, in the studies reporting VB strength for the other NIA-supported rodent strains (Table 1), correlations between strength and VB characteristics were not tested for significance as has been done for human lumbar VBs [20–22]. Thus, it is not known if the age-related decrease in the BV/TV or aBMD of mouse vertebrae is the primary reason for the decrease in VB strength.

In order to validate a preclinical model of the age-related increase in fracture risk of the lumbar vertebral body for studies in which the primary objective is to assess the efficacy of a new therapeutic strategy for preventing vertebral fractures, we characterized the difference in trabecular architecture of the L6 VB between 6-mo. and 20-mo. BALB/c mice and tested whether the strength of the L6 VB in compression was actually lower with age for both females and males representing young adulthood (~24% and ~26% of typical lifespan, respectively) and old age (~80% and ~86% of typical lifespan, respectively) [23]. The characterization of trabecular bone was done with respect to the distal femur metaphysis to ascertain whether long bones can serve as a surrogate of the vertebrae with respect to trabecular architecture. Since the strength of human lumber VBs decreases with age [24] and since volumetric BMD is a reported predictor of compressive strength of cadaveric VBs [25], we hypothesized that strength of the murine lumbar VB also decreases between young adulthood (6-mo.) and old age (20-mo.) and that the age-related decrease in volumetric BMD (or BV/TV) explains the decrease in VB strength. In addition, since micro-computed tomography (μCT) scans of bone can readily be converted to finite element (FE) models for a linear elastic analysis of the stress and strain experienced by the bone, we also determined whether the prediction of VB strength by a μCT-derived FE analysis (μFEA) of each mouse L6 VB significantly correlated with the experimental measurement of VB strength. This was done in comparison with other potential μCT-derived predictors of VB strength.

2. Materials and Methods:

2.1. Age groups and VB collection

We acquired male BALB/c mice at 19 months of age (n=20) and at 2 months of age (n=20) from Charles River Laboratories, which maintains an aging colony with support from the NIA. Separately, we acquired female BALB/c mice at 19 months of age (n=20) and at 4–5 months of age (n=20) from the same source. All mice were fed a standard rodent chow (5L0D, LabDiet, St Louis, MO) *ad libitum* while being housed in non-sterile, micro-isolator cages during a 12-hour light/dark cycle until reaching 6 months or 20 months of age. For both the males and females, two of the older mice died before reaching 20 months leaving 20 young adult and 18 old mice within each sex. Euthanasia involved cervical dislocation following cardiac exsanguination while the mouse was under deep anesthesia (ketamine at 100 mg/kg + xylazine at 10 mg/kg). These procedures were approved by the Vanderbilt University Medical Center IACUC. Following dissection and cutting through intravertebral discs, the L5 and L6 VBs were immersed in phosphate buffered saline (PBS) and stored at −20 °C.

2.2. Micro-computed tomography (μCT) analysis

With cranial-caudal axis or the long axis vertically aligned with the scanner tube, each L6 vertebra or distal femur metaphysis, respectively, were imaged in PBS using a high-resolution μCT scanner (μCT40; Scanco Medical AG, Brüttisellen, Switzerland). For both bones, the scan parameters were: 70 kVp/200 μA, 0.5 mm Al filter, beam-hardening correction, 500 samples per 1000 projections per full rotation, 300 ms integration time, and 12 μm isotropic voxel size. To initially define the region of interest (ROI) of the L6 VBs for assessing trabecular bone, contours were first drawn by hand within multiple image slices between the cartilaginous end-plates and morphed to add contours in the 10 intervening slices (Fig. 1A). To separate the trabecular bone from the cortex of the distal femur metaphysis, an auto-contouring algorithm [26] was used with the following input parameters: outer threshold = 2826.0 mgHA/cm^3, inner threshold = 561.1 mgHA/cm^3, dilate cortex = 10, dilate marrow = 6, minimum cortical thickness = 6, discard minimum cortex pore = 2, trabecular peel iteration = 3, gap of inner cortex contour to trabecular border =1. Applying the manufacturer's built-in Gaussian filter with a support of 1 (kernel size of blurring) and a sigma of 0.2 (variance of the Gaussian point spread function) to suppress image noise, a global threshold of 235 per mille in which mille is the native unit of attenuation (383.3 mgHA/cm^3 based on hydroxyapatite calibration) segmented the trabecular bone from air and soft tissue (Fig. 1A) in each L6 VB. To segment the trabecular bone in the distal femur, the parameters of the Gaussian image blurring algorithm were a support of 2.0 and a sigma of 0.2. The global threshold was 240 per mille (536.0 mgHA/cm^3). Applying the Scanco script for trabecular bone evaluations, standard architectural parameters (BV/TV, Tb.N, etc.) were determined. Moreover, using the calibration to a hydroxyapatite (HA) phantom to convert native attenuation levels to mgHA/cm^3, the tissue mineral density of trabecular bone (Tb.TMD) was determined as the mean TMD among all bone voxels after peeling 2 voxels from the surface (to suppress partial volume effects). The apparent volumetric bone mineral density of trabecular bone (Tb.vBMD) was the mean of all voxels within the centrum (Fig. 1A).

2.3. Evaluations of the thin cortex

To isolate the thin cortex of the L6 centrum as well as to generate finite element (FE) models of each VB, a circle with a constant radius of 1.24 mm (for female mice) and 1.15 mm (for male mice) was copied into each slice of the image stack between the end plates and positioned to transect the transverse processes (Fig. 1B), which did not bear load in the *quasi*-static compression tests. Again, image noise was suppressed using a Gaussian filter with a sigma of 0.2 and support of 1, and bone was segmented from soft tissue and air using a global threshold of 235 per mille (Fig. 1B). Next, the three-dimensional (3D), segmented image of the trabecular bone (Fig. 1A, Fig. S1A) was subtracted from the 3D, segmented image of the whole VB within the circle and between the end-plates (Fig. 1B, Fig. S1B) to produce a 3D, segmented image of the thin cortex (Fig. 1C, Fig. S1C). This cortex was evaluated using the Scanco mid-shaft script to determine shell thickness (Sh.Th), cross-sectional area of the shell (Sh.Ar), and shell TMD (Sh.TMD). The cortex of the distal femur, as defined by the auto-contouring algorithm (Fig. S2 and S3), was also evaluated with the mid-shaft script using a global threshold of 666.8 mgHA/cm^3 (support of 1.0 and sigma of 0.2) to determine the total cross-sectional area, thickness, porosity (1 - BV/TV), and tissue mineral density of the metaphyseal cortex (Met.Tt.Ar, Met.Th, Met.Po, and Met.TMD, respectively).

2.4. μCT-derived finite element analysis (μFEA)

Following the methods described in our previous paper [27], the compressive strength of L6 VBs was predicted using linear elastic μFEA. Briefly, Scanco FE-software (v1.13, Scanco Medical AG, Brüttisellen, Switzerland) was used to directly convert isotropic bone voxels to 8-node, hexahedral elements. Then, element-wise strain values (Fig. S4) were determined for boundary conditions that simulated high-friction, axial compression loading of each VB to a peak apparent strain of 1%. That is, the caudal nodes were constrained in the x-, y- and z-direction, and the cranial nodes were constrained in x- and y-direction with a defined negative displacement in the z-direction. In one μFEA (homogenous), all elements were assigned an elastic tissue modulus (E_t) and a Poisson's ratio (ν) equal to 18 GPa and 0.3, respectively. In another μFEA (inhomogeneous), individual voxels were binned into 40–42 materials based on their attenuation value (bin = 23.6–23.7 mgHA/cm^3). The E_t of each material was determined using a relationship derived by Easley et al. ($E_t = 0.1127 \times TMD^{1.746}$; MPa from mgHA/cm^3) [28]. Following the linear failure criteria from Pistoia et al. [29], the reaction force at which 2% of the model volume exceeded an equivalent strain of 0.007 was the predicted strength.

2.5. Compression testing of the L6 vertebral body (VB)

A curved micro-serrated surgical scissor was used to snip the inferior articular processes and distal end of the spinous process exposing the intervertebral foramen. The superior articular processes were also carefully cut while ensuring that the specimen remained intact so that the VB was the only portion to bear the load during the compression test. Each L6 VB was then rehydrated and positioned between a pair of stainless-steel compression rods (outer diameter 1.97 mm) mounted to the chucks of a material testing frame (Instron Dynamight 8841, Norwood, MA). The lower compression platen supports a moment relief to ensure

pure axial compression of the VB during test (Fig. S5). The hydrated VB was pre-loaded to 2 N and then loaded-to-failure at a rate of 3.0 mm/min. The load and displacement data were recorded at a sampling rate of 50 Hz by force transducer with maximum capacity of 100 N (Honeywell, Morristown, NJ, USA) and the linear variable displacement transducer (Dynamight 8841, Instron, Canton, OH), respectively. The VB strength was the ultimate force to failure.

2.6. Statistical Analysis

Within each sex, we tested the null hypothesis that a bone property was not different between the 2 age groups using a two-sided t-test with Welch's correction. In the event that values of a given property did not come from a Gaussian distribution (D'Agostino-Pearson omnibus normality test with an $\alpha = 0.05$) for one of the age groups, the Mann-Whitney U test was used. Linear regressions between maximum force and selected VB parameters of interest as well as characteristics of distal femur metaphysis were performed (females separate from males) to determine whether one straight line fit the data or two straight lines, one for each age group, fit the data using Akaike's information criterion. The choice was based on the probability being greater than 70%. When the probability was less than 70%, data was fit both ways, combined and separate. Normality and homoscedasticity of the residuals for all linear regressions were checked using the D'Agostino-Pearson test and the test for appropriate weighting (i.e., no correlation between the Y value from the linear equation and the absolute value of the residual). Since one of these tests failed for most of the regressions involving the female data, we report Spearman correlations for female mice and Pearson correlations for male mice (unless otherwise noted). All preceding statistical analyses were done using GraphPad Prism (v8.3.0, GraphPad Software, La Jolla, CA). For the linear regressions involving metaphyseal characteristics in which residuals did not pass normality or homoscedasticity, data was bootstrapped (500 replicates) to obtain the p-value for the slope = 0. To determine which bone parameters best explained VB strength for all the data pooling males and females, bootstrapped (500 replicates) general linear models (GLMs) were used to first determine whether the association between ultimate force and the selected bone parameter was independent of age group and sex of the mice. In a backwards stepwise manner, non-significant interaction terms ($p<0.05$) were removed and then non-significant ($p<0.05$) covariates (age and/or sex) were removed. Next, bootstrapped GLMs were used to determine if a second bone variable could improve the prediction of VB strength.

3. Results:

3.1. Between 6-months and 20-months of age, there was a deterioration in the architecture of trabecular bone within the distal femur metaphysis

Confirming previous preclinical studies of aging mice [15,18,30,31], the amount and apparent volumetric bone mineral density of trabecular bone (Tb.vBMD) decreased between adulthood (6-mo.) and old age (20-mo.) in the distal femur metaphysis of female and male BALB/c mice (Table 2, Fig. 2). Specifically, trabecular bone volume fraction (BV/TV) and Tb.vBMD was, on average, 60.9% and 49.5% lower, respectively, with age for female mice and 20.2% and 11.5% lower, respectively, with age for male mice. Most of the architectural characteristics of trabecular bone deteriorated between 6-mo. and 20-mo., regardless of the

sex of the animal (Table 2). One exception among the female mice was the lack of a significant difference in trabecular thickness (Tb.Th) between the 2 age groups, and one exception among the male mice was the lack of a significant difference in structural model index (SMI) between the age groups. While the Tb.vBMD decreased with age, the tissue mineral density of trabecular bone (Tb.TMD) was significantly higher at 20-mo. compared to 6-mo. (Female: 5.5% on average and Male: 3.2% on average).

With respect to the cortex of the distal femur above the growth plate (Fig. S1 and S2), there were additional age-related changes in the male bone. The total cross-sectional area of the metaphyseal cortex (Met.Tt.Ar), the thickness of this cortical bone (Met.Th), and porosity (Met.Po) was lower at 20-mo. than at 6-mo. Such age-related changes were not observed between 6-mo. and 20-mo. female BALB/c mice. As with the trabecular bone of the metaphysis, the tissue mineral density of the metaphyseal cortex (Met.TMD) increased with age in both male and female mice.

3.2. BV/TV of the trabecular bone within the L6 VB decreased between 6-mo. and 20-mo. in male mice

Unlike the age-related decrease in trabecular bone of the distal femur metaphysis, the BV/TV and Tb.vBMD within the L6 centrum was significantly lower by 12.6% and by 9.5% on average, respectively, between 6-months and 20-months of age for only the male BALB/c mice (Fig. 3). There were however a few architectural characteristics of lumbar VB trabecular bone that deteriorated with age in both sexes of mice, namely a loss in trabecular number (Tb.N), a loss in connectivity density (Conn.D), and an increase in trabecular spacing (Tb.Sp) (Table 3). A thinning of the trabeculae over the selected age range only occurred in the male mice (Table 3). The age-related increase in Tb.TMD of the L6 VB was only significant for the male mice (Table 3).

The trabecular bone within centrum is not the sole contributor to the compressive strength of the VB as a thin cortex surrounds this bone and bears axial loads. Upon isolating the cortex of the centrum for evaluation of its structure (Fig. 1 and Fig. S3), the shell cross-sectional area (Sh.Ar) was lower with age for the male mice but not for the female mice (Table 3). Rather, the shell thickness (Sh.Th) decreased between 6-mo. and 20-mo. in only the female mice. Unlike the other sites, the tissue mineral density of the shell (Sh.TMD) did not change with age. The TMD of the entire L6 VB without the transverse processes was higher at 20-mo. than at 6-mo, irrespective of the sex of the animal. Also, similarly across females and males, the bone cross-sectional area of VB (B.Ar) did not change with age but the axial length (Ax.Le) increased with age (significantly in males only).

3.3. Compressive strength of the male L6 VB was lower at 20-mo. than at 6-mo.

For the male BALB/c mice, the ultimate force experienced by the L6 VB was lower at 20-mo. than at 6-mo. of age (Fig. 4). With respect to the female mice, there was no age-related difference in compressive strength of this VB at the whole-bone level. Upon accounting for differences in the bone cross-sectional area between the age groups (normalized force by B.Ar, not total area), the ultimate stress was still lower for old male mice than for the young adult male mice (again, no difference in the females). Interestingly, the linear elastic,

homogeneous material model predicted an age-related decrease in VB strength, whereas the inhomogeneous or heterogeneous material model predicted no difference in VB strength, irrespective of the sex of the BALB/c mouse (Fig. 4).

3.4. Trabecular bone volume fraction and volumetric bone mineral density positively correlated with the ultimate compressive force of the L6 VB, regardless of the sex of the animal.

For both female and male mice, trabecular BV/TV and vBMD directly correlated with the ultimate force of the L6 VB in compression (Table 4). The strength of these correlations was higher and lower than the strength of the μFEA-derived correlations for the female and male mice, respectively. Combining the age groups, Tb.N and B.Ar also directly correlated with ultimate force of female mice only. The relationships between Tb.N and ultimate force and between B.Ar and ultimate force were different between the age groups for the male mice, and so correlations were separately tested for significance. For 20-mo. male mice, B.Ar directly correlated with ultimate compressive force with the strength of the correlation being similar to those for μFEA predictions (Table 4). As for the 6-mo. male mice, few μCT-derived properties correlated with ultimate compressive force. One exception was weak correlation between VB strength and Ax.Le. Pooling all 4 groups, the ultimate force of the L6 VB directly correlated with BV/TV, Tb.avBMD, Sh.Th, and B.Ar (Table S1), regardless of whether sex or age is a significant covariate.

3.5. Assessing the micro-structure and bone mineral density of the distal femur metaphysis does not provide surrogates for age-related changes in VB strength.

Unlike BV/TV of the L6 VB, BV/TV of the distal femur metaphysis was not linearly related to the ultimate compressive force of the L6 VB in the regression analysis of female bones (Fig. S6A), and the linear relationship in the regression analysis of male bones was rather weak (R^2=0.128, p=0.028) when combining the 2 age groups (Fig. S6A). Other selected characteristics of the distal femur metaphysis such as Tb.N (Fig. S6B), Tb.vBMD (Fig. S6C), plate- vs. rod-like structure or SMI (Fig. S7A), Conn.D (Fig. S7B), and Met.Po (Fig. S7C) were also not linearly related to VB strength. Trabecular thickness (Fig. S6D) and thickness of the metaphyseal cortex (Fig. S7D) were the only characteristics of the distal femur to significantly explain some of the variance in ultimate compressive force of both female and male VBs. The predictive ability of these characteristics however was rather weak (R^2 values between 0.151 and 0.271, $p<0.05$) when combining the 2 age groups. Lastly, different curves for each age group was more representative of these linear relationships than a single curve involving the male data (Fig. S6 and S7).

3.6. μFEA predictions of strength and other μCT-derived predictors are not necessarily independent of age or sex.

To identify which bone parameter best predicts the whole-bone strength of the mouse L6 VB (ultimate compressive force), we fit the data from all mice to GLMs starting with 2 covariates, age group and sex. The predicted failure strength as determined by μFEA depended on age but not on the sex of the mice (Table 5). Moreover, the interaction between predicted failure strength and age group was significant such that the slope of the linear regression was higher for the 20-mo. than for the 6-mo. old mice. This was the case

regardless of a homogeneous (HM) distribution of modulus (Fig 5A) or a heterogeneous (HT) distribution of modulus (Fig 5B). The HT-FE model did not improve the prediction of VB strength. To test the robustness of the predictions, the significance of the GLMs were repeatedly tested for all combinations of N=74 (leaving 2 mice out each time). Of the 2,851 possible regressions using the data from HM-μFEA as the explanatory variable (Supplemental Materials), 4.91% had a p-value greater than 0.05 for the predicted failure (i.e., slope), but the interaction with age group was still significant ($p<0.004$). As for the interaction between predicted strength and age group (i.e., difference in slope), 0.14% had a p-value between 0.0501 and 0.0734. When using the data from HT-μFEA, the values for the predicted failure force and interaction term increased to 9.93% and 0.18% (p-value between 0.0505 and 0.1015), respectively. Thus, the age-related difference in the relationship between the ultimate force from compression testing and the predicted failure force from the two FE models (Fig. 5) is likely real.

Neither sex nor age group were significant covariates of trabecular BV/TV meaning one straight line significantly related BV/TV to the ultimate compressive force of the L6 VB (VB strength), not multiple straight lines for each group. The association between Tb.vBMD and VB strength also did not depend on age group, but this linear relationship was different between females and males such that for a given volumetric bone mineral density, the female VB was stronger than the male VB. As might be expected from the observation that Tb.N correlated with VB strength for female mice only, there were significant interactions between sex of the animal and age group and between Tb.N and sex of the animal (Table 5). In effect, Tb.N was a positive contributor to VB strength in female mice only. The cross-sectional bone area (B.Ar), as an explanatory variable of VB strength, was similar to the μFEA predictions in that the slope of the linear regression was higher for the 20-mo. than for the 6-mo. old mice (Table 5). When combining Tb.vBMD and B.Ar, age group and sex were no longer significant covariates, and the predictive ability of these two explanatory variables (adj-R^2 = 0.3985) was similar to each variable alone when including the covariate (adj-R^2 = 0.3972 for Tb.vBMD + Sex and = 0.4062 for B.Ar + Age). Unlike Tb.vBMD, B.Ar did not help BV/TV predict VB strength.

4. Discussion:

To continue developing effective osteoporosis medications with minimal side effects, therapeutic strategies to treat osteoporosis would include reversing the age-related decrease in VB strength, not just the decrease in bone mass or areal BMD that occurs with the onset of sex steroid deficiency, since fragility fracture are most prevalent among the elderly. Towards that end, male BALB/c mice phenocopy the decline in whole VB strength with aging that occurs in humans when comparing strength measurements between 6-mo. and 20-mo. old BALB/c mice. As such, the efficacy of a therapeutic strategy to increase the compressive strength of the lumbar VB to the level that occurs in young adulthood can be tested in this NIA-supported, preclinical model of aging. The ability of a therapeutic strategy to increase VB strength can also be tested in female BALB/c mice; but the findings of present study cannot indicate the degree to which strength must be improved to restore peak VB strength since there was not a significant difference in the ultimate compressive force of the female L6 VB between 6-mo. and 20-mo. of age. Nonetheless, independent of the sex of

the animal, trabecular BV/TV appears to be the primary determinant of VB strength in mice followed by the combination of trabecular vBMD and bone cross-sectional area of the VB (Table 5). A therapeutic strategy to increase mineralization or tissue mineral density would likely not be suitable for testing in the BALB/c model of aging because TMD of the lumbar VB increases with age in both male and female mice.

There are similarities and discrepancies in the aging phenotype of the lumbar VB between the present study and the previous study involving female and male BALB/c mice spanning multiple ages (2-, 4-, 7-, 12-, and 20-mo.) by Willinghamm et al. Trabecular BV/TV of the L5 VB was 9.2% (female) and 8.5% (male) lower in the 20-mo. than in the 7-mo. age group, but the difference was not statistically significant [18]. In the present study, trabecular BV/TV of the L6 VB was 1.7% (female) and 12.6% (male) lower in the 20-mo. than in the 6-mo. age group with the difference being statistically significant in male mice only. Trabecular number and spacing were significantly lower and higher, respectively, with age, regardless of the sex of the animal, in both studies. The previous study found that trabecular thickness did not change with age in male and female mice, whereas the present study found a significant decrease in Tb.Th with age in male mice only. Consistent across studies though, volumetric BMD of the trabecular bone within the centrum decreased with age in the male BALB/c mice but not in the female BALB/c mice (Table 3). Accompanying the age-related decrease in Tb.vBMD in the male mice, there was a significant 25.6% decrease in ultimate force of the L5 VB between 7-mo. and 20-mo. of age in the previous study [18] and a significant 18.7% decrease in ultimate force of the L6 VB between 6-mo. and 20-mo. of age in the present study. Willinghamm et al. also reported a significant 22.2%–22.6% decrease in ultimate force of the L5 VB between 7-mo. and 20-mo. as well as between 12-mo. and 20-mo. of age for the female BALB/c mice. Moreover, Trabecular BV/TV and Tb.vBMD was highest at 12-mo. of age in the females in the previous study, while these characteristics did not change between 7-mo. and 12-mo. of age in the males [18]. It would appear then that male BALB/c mice attain peak bone mass and strength of the lumbar vertebrae at an earlier age than female BALB/c mice (~6–7-mo. compared to ~12-mo.) and that male mice lose compressive strength at a younger age than female mice (between 6- and 12-mo. compared to an age between 12- and 20-mo., respectively).

Like human VBs [32,33], the compressive strength of the mouse L6 VB directly correlates with vBMD for both females and males (Table 4). When pooling all mice (N=76), trabecular BV/TV is independent of age and sex of the animal explaining 40.7% of the variance in ultimate compressive force; whereas, the contribution of Tb.vBMD to ultimate force is different between males and females (Table 5). This is likely due to a sex-related difference in the bone cross-sectional area of the L6 VB because sex is no longer a significant covariate when B.Ar is added to the linear regression model (Table 5) in which the combination of Tb.vBMD and B.Ar explain 39.9% of the variance in ultimate force. There are likely a number of factors then that osteoporosis therapies could improve to increase VB strength beyond BV/TV, Tb.vBMD, and B.Ar. Two possibilities include trabecular number for female mice and shell thickness of the VB for male as these two structural characteristics of the VB correlated with ultimate force (Table 4).

Assessing changes or differences in the distal femur metaphasis of mice is likely not a suitable surrogate for the changes or differences that occur in the lumbar spine of mice. In addition to the higher percent difference in BV/TV between 6-mo. and 20-mo. that occurred within the metaphysis compared to the percent difference within the centrum of the L6 for both female and male mice, the age-related change in Tb.N was not consistent across anatomical sites. For female mice, there was 37.6% decrease in Tb.N within the metaphysis compared to a 14.2% decrease within the VB. On the other hand, the age-related decrease in Tb.N was similar between the metaphysis (8.3%) and the L6 centrum (6.3%) in male mice, but Tb.N for either bone was not related to the age-related decrease in VB strength (Table 4 and Fig. S6B) that was observed in males. Predicting treatment effects on VB fracture risk in the context of pre-clinical models of aging from assessments of distal femur metaphysis is seemingly not advisable given the lack of significant associations (or weak associations) between characteristics of the distal femur morphology and VB compressive strength for both female and male mice (Fig. S6 and S7).

The advantage of μCT-derived finite element analysis (μFEA) is its ability to provide an estimate of the failure force without destroying the VB sample or sacrificing the animal in the case of *in vivo* μCT. Of the preclinical studies that used μFEA to assess the effect of therapy on the compressive strength (or stiffness) of bone, the majority did not compare predictions of bone strength to mechanical measurements of bone strength: cubic volume of trabecular bone within tibia metaphysis [34,35], trabecular compartment of the tibia metaphysis [36,37], whole L2 VB and trabecular compartment within the centrum [28], whole L5 VB [38], whole L4 VB [39–41], whole L6 VB including load distribution between cortical shell and inner trabecular bone [42], distal femur [43], and lastly a section of the proximal diaphysis of the tibia including cortical and trabecular bone [44]. Of the preclinical studies that compared μFEA predictions and experimental measurements from mechanical tests, two involved strength analysis of the proximal femur or the distal femur. Takao-Kawabata et al. reported a significant correlation between predicted failure load of proximal femur (female rats) and ultimate load experienced by the proximal femur when the femoral head was loaded in compression ($r = 0.574$, $p<0.01$ pooling all treatment groups) [45]; and Wernle et al. reported a significant correlation between predicted failure load of the distal femur in compression and experimentally determined failure load ($R^2 = 0.46$ for irradiated bones and $R^2 = 0.71$ for the control bones using embrittled material behavior in which yield stress is nonlinear function of TMD) [46]. In our previous studies involving mouse VB strength and a similar linear failure criteria as the present study, we found significant correlations between ultimate compressive force for the L6 VB and the predicted failure force when pooling control antibody (13C4)-treated mice and anti-transforming growth factor beta antibody (1D11)-treated mice ($R^2 = 0.623$ to 0.703 depending on homogeneous or heterogeneous material definition) [27], when pooling mice lacking activating transcription factor 4 (*Atf4*−/−) and wild-type (*Atf4*+/+) littermates ($R^2 = 0.838$ to 0.887 depending on homogeneous or heterogeneous material definition) [27], and when pooling 4 treatment groups (13C4, 1D11, bortezomib, and 1D11+bortezomib) in a mouse model of multiple myeloma-induced bone disease ($R^2 = 0.737$ using the heterogeneous material definition) [47]. Despite these strong correlations between μFEA predictions and experimental measurements involving relatively young mice (<4-mo. of age), the findings of

the present study (Table 5 and Fig. 5) suggest that this numerical method is not a surrogate of strength measurements from mechanical testing in the context of age-related changes in VB strength.

There are potentially other age-related changes in the bone matrix of the lumbar VB - documented in our previous study of the long bones of BALB/c mice [48] - contributing to the decline in VB strength between 6-mo. and 20-mo. old male mice. Supporting this supposition, the linear relationship between ultimate compressive force and predicted failure force was best explained by 2 regression lines, one for each age group (Table 4). Even when the data from the female mice was pooled with the data from the male mice, there was still a significant interaction between age group and predicted failure force (Table 5) meaning the slopes of the regression lines were different between young and old VBs (Fig. 5). In effect, μFEA is overestimating the strength of lumbar VBs from old mice.

Unexpectedly, the heterogeneous distribution of modulus did not improve the ability of μFEA to predict VB strength as expected. With a fixed homogeneous distribution of tissue modulus (e.g., E_t = 18 GPa for all FE models) that does not depend on the mean TMD of the bone, the predicted failure force primarily depends on structure or morphometry of the bone for a given linear elastic, failure criteria. When the modulus of tissue is a function of tissue mineral density (e.g., partitioned into 40 to 42 materials based on TMD), the predicted failure force depends on both morphometry and the positive contribution of mineralization to bone strength. In effect, the heterogeneous μFEA predicted that the age-related increase in the TMD of the whole VB would offset the age-related decrease in the trabecular BV/TV in the male BALB/c mice. That VB strength was actually lower with age supports the supposition that the quality of bone matrix degraded between 6-mo. and 20-mo. of age. While heterogenous modulus distribution improves the ability of μFEA to predict apparent stiffness of trabecular bone (as reviewed in [49]), it does not necessarily improve the prediction of whole bone strength (e.g., strength of cadaveric radius during a fall [50]), at least not when using linear fracture criteria in which the volume threshold of failure (e.g., 2%) does not depend on the variance of tissue modulus.

In addition to the assessment of VB strength for 2 age groups, which precluded establishing peak ultimate compressive force for female mice, the limitations of the present study included i) generating FE models from μCT scans acquired before removing the transverse processes (digitally removed), ii) investigating one set of failure criteria (linear: 2% tissue volume exceeding 0.007 equivalent strain), and iii) having only one matrix characteristic (TMD from a polychromatic X-ray source). While the vertical alignment of VB scan was checked prior to voxel-to-element conversion, the boundary conditions of the FE model did not precisely match the compressive loading of VBs by the 2 platens of the mechanical testing system. Possibly, the use of a non-linear failure criteria (e.g., linear elastic-perfectly plastic constitutive material behavior with asymmetry) may improve the prediction of the VB failure force. Other assessment techniques that characterize the organic matrix of bone may also help explain why VB strength decreased as the male mice aged from 6-mo. to 20-mo. The effect sizes of the bone measurements reported herein are available to power such studies (Table S2).

5. Conclusions

In the BALB/c model of aging, the compressive strength of the L6 vertebra at the whole-bone level decreased between 6-mo. and 20-mo. for male mice but not for female mice. Trabecular bone volume fraction and the combination of volumetric BMD and bone cross-sectional area of the VB are likely determinants of mouse VB strength. While the non-destructive, μCT-derived finite element analysis with linear-based failure criteria can predict the failure force of the L6 VB, it does not appear to be suitable surrogate of strength measurements from mechanical testing with respect to aging effects on VB strength. Moreover, the age-related deterioration in trabecular architecture was more pronounced within distal femur metaphysis than within the VB centrum, irrespective of the sex of the mouse. The BALB/c mouse strain is a suitable preclinical model to investigate the efficacy of new osteoporosis therapies developed to combat the age-related increase in the risk of vertebral body fractures.

Supplementary Material

Refer to Web version on PubMed Central for supplementary material.

Acknowledgements

This work was funded in part by a training grant from NIDDK (DK101003) and by grants from the National Institute of Arthritis and Musculoskeletal and Skin Diseases (AR067871) and the Department of Veterans Affairs (VA), Veterans Health Administration, Office of Research and Development (1I01BX001018). The use of the micro-computed tomography scanner (μCT50) was made possible by a National Institutes of Health (NIH) grant (S10RR027631-01). The content provided herein does not necessarily reflect the views of NIH or VA.

Grant Supporters: NIDDK, NIAMS, VA, NIH.

References

[1]. Johnell O, Kanis JA, An estimate of the worldwide prevalence and disability associated with osteoporotic fractures, Osteoporos Int. 17 (2006) 1726–1733. doi:10.1007/s00198-006-0172-4. [PubMed: 16983459]

[2]. McCabe E, Ibrahim A, Singh R, Kelly M, Armstrong C, Heaney F, et al., A systematic review of the Irish osteoporotic vertebral fracture literature, Arch Osteoporos. 15 (2020) 136–9. doi:10.1007/s11657-020-0704-0.

[3]. Glaser DL, Kaplan FS, Osteoporosis. Definition and clinical presentation, Spine. 22 (1997) 12S–16S. doi:10.1097/00007632-199712151-00003. [PubMed: 9431639]

[4]. Wright NC, Looker AC, Saag KG, Curtis JR, Delzell ES, Randall S, et al., The Recent Prevalence of Osteoporosis and Low Bone Mass in the United States Based on Bone Mineral Density at the Femoral Neck or Lumbar Spine, J Bone Miner Res. 29 (2014) 2520–2526. doi:10.1002/jbmr.2269. [PubMed: 24771492]

[5]. Lei T, Liang Z, Li F, Tang C, Xie K, Wang P, et al., Pulsed electromagnetic fields (PEMF) attenuate changes in vertebral bone mass, architecture and strength in ovariectomized mice, Bone. 108 (2018) 10–19. doi:10.1016/j.bone.2017.12.008. [PubMed: 29229438]

[6]. Bahar H, Gallacher K, Downall J, Nelson CA, Shomali M, Hattersley G, Six Weeks of Daily Abaloparatide Treatment Increased Vertebral and Femoral Bone Mineral Density, Microarchitecture and Strength in Ovariectomized Osteopenic Rats, Calcif Tissue Int. 99 (2016) 489–499. doi:10.1007/s00223-016-0171-1. [PubMed: 27395059]

[7]. Ucer S, Iyer S, Kim H-N, Han L, Rutlen C, Allison K, et al., The Effects of Aging and Sex Steroid Deficiency on the Murine Skeleton Are Independent and Mechanistically Distinct, J Bone Miner Res. 32 (2016) 560–574. doi:10.1002/jbmr.3014. [PubMed: 27714847]

[8]. Melton LJ, Kan SH, Frye MA, Wahner HW, O'Fallon WM, Riggs BL, Epidemiology of vertebral fractures in women, Am. J. Epidemiol 129 (1989) 1000–1011. doi:10.1093/oxfordjournals.aje.a115204. [PubMed: 2784934]

[9]. Mosekilde L, Age-related changes in vertebral trabecular bone architecture--assessed by a new method, Bone. 9 (1988) 247–250. [PubMed: 3048340]

[10]. Crawford RP, Cann CE, Keaveny TM, Finite element models predict in vitro vertebral body compressive strength better than quantitative computed tomography, Bone. 33 (2003) 744–750. doi:10.1016/S8756-3282(03)00210-2. [PubMed: 14555280]

[11]. Christiansen BA, Kopperdahl DL, Kiel DP, Keaveny TM, Bouxsein ML, Mechanical contributions of the cortical and trabecular compartments contribute to differences in age-related changes in vertebral body strength in men and women assessed by QCT-based finite element analysis, J Bone Miner Res. 26 (2011) 974–983. doi:10.1002/jbmr.287. [PubMed: 21542000]

[12]. Uppuganti S, Granke M, Makowski AJ, Does MD, Nyman JS, Age-related changes in the fracture resistance of male Fischer F344 rat bone, Bone. 83 (2016) 220–232. doi:10.1016/j.bone.2015.11.009. [PubMed: 26610688]

[13]. Wang L, Banu J, McMahan CA, Kalu DN, Male rodent model of age-related bone loss in men, 29 (2001) 141–148.

[14]. Bar-Shira-Maymon B, Coleman R, Cohen A, Steinhagen-Thiessen E, Silbermann M, Age-related bone loss in lumbar vertebrae of CW-1 female mice: a histomorphometric study, 44 (1989) 36–45.

[15]. Glatt V, Canalis E, Stadmeyer L, Bouxsein ML, Age-related changes in trabecular architecture differ in female and male C57BL/6J mice, 22 (2007) 1197–1207. doi:10.1359/jbmr.070507.

[16]. Almeida M, Han L, Martin-Millan M, Plotkin LI, Stewart SA, Roberson PK, et al., Skeletal involution by age-associated oxidative stress and its acceleration by loss of sex steroids, J Biol Chem. 282 (2007) 27285–27297. doi:10.1074/jbc.M702810200. [PubMed: 17623659]

[17]. Illien-Junger S, Palacio-Mancheno P, Kindschuh WF, Chen X, Sroga GE, Vashishth D, et al., Dietary Advanced Glycation End Products Have Sex- and Age-Dependent Effects on Vertebral Bone Microstructure and Mechanical Function in Mice, J Bone Miner Res. 33 (2017) 437–448. doi:10.1002/jbmr.3321. [PubMed: 29160901]

[18]. Willinghamm MD, Brodt MD, Lee KL, Stephens AL, Ye J, Silva MJ, Age-related changes in bone structure and strength in female and male BALB/c mice, 86 (2010) 470–483. doi:10.1007/s00223-010-9359-y.

[19]. LaMothe JM, Hepple RT, Zernicke RF, Bone adaptation with aging and long-term caloric restriction in Fischer 344 x Brown-Norway F1-hybrid rats, J. Appl. Physiol 95 (2003) 1739–1745. doi:10.1152/japplphysiol.00079.2003. [PubMed: 12807893]

[20]. McBroom RJ, Hayes WC, Edwards WT, Goldberg RP, White AA, Prediction of vertebral body compressive fracture using quantitative computed tomography, J Bone Joint Surg Am. 67 (1985) 1206–1214. [PubMed: 4055845]

[21]. Cody DD, Goldstein SA, Flynn MJ, Brown EB, Correlations between vertebral regional bone mineral density (rBMD) and whole bone fracture load, Spine. 16 (1991) 146–154. [PubMed: 2011769]

[22]. Maquer G, Lu Y, Dall'Ara E, Chevalier Y, Krause M, Yang L, et al., The Initial Slope of the Variogram, Foundation of the Trabecular Bone Score, Is Not or Is Poorly Associated With Vertebral Strength, (2015) n/a–n/a. doi:10.1002/jbmr.2610.

[23]. Yuan R, Tsaih S-W, Petkova SB, Marin de Evsikova C, Xing S, Marion MA, et al., Aging in inbred strains of mice: study design and interim report on median lifespans and circulating IGF1 levels, Aging Cell. 8 (2009) 277–287. doi:10.1111/j.1474-9726.2009.00478.x. [PubMed: 19627267]

[24]. Kurutz M, Donáth J, Gálos M, Varga P, Fornet B, Age- and sex-related regional compressive strength characteristics of human lumbar vertebrae in osteoporosis, J Multidiscip Healthc. 1 (2008) 105–121. [PubMed: 21197342]

[25]. Ebbesen EN, Thomsen JS, Beck-Nielsen H, Nepper-Rasmussen HJ, Mosekilde L, Lumbar vertebral body compressive strength evaluated by dual-energy X-ray absorptiometry, quantitative computed tomography, and ashing, Bone. 25 (1999) 713–724. doi:10.1016/s8756-3282(99)00216-1. [PubMed: 10593417]

[26]. Buie HR, Campbell GM, Klinck RJ, Macneil JA, Boyd SK, Automatic segmentation of cortical and trabecular compartments based on a dual threshold technique for in vivo micro-CT bone analysis, 41 (2007) 505–515. doi:10.1016/j.bone.2007.07.007.

[27]. Nyman JS, Uppuganti S, Makowski AJ, Rowland BJ, Merkel AR, Sterling JA, et al., Predicting mouse vertebra strength with micro-computed tomography-derived finite element analysis, Bonekey Rep. 4 (2015) 1–11. doi:10.1038/bonekey.2015.31.

[28]. Easley SK, Jekir MG, Burghardt AJ, Li M, Keaveny TM, Contribution of the intra-specimen variations in tissue mineralization to PTH- and raloxifene-induced changes in stiffness of rat vertebrae, 46 (2010) 1162–1169. doi:10.1016/j.bone.2009.12.009.

[29]. Pistoia W, van Rietbergen B, Lochmüller E-M, Lill CA, Eckstein F, Rüegsegger P, Estimation of distal radius failure load with micro-finite element analysis models based on three-dimensional peripheral quantitative computed tomography images, 30 (2002) 842–848.

[30]. Halloran BP, Ferguson VL, Simske SJ, Burghardt A, Venton LL, Majumdar S, Changes in bone structure and mass with advancing age in the male C57BL/6J mouse, J Bone Miner Res. 17 (2002) 1044–1050. doi:10.1359/jbmr.2002.17.6.1044. [PubMed: 12054159]

[31]. Courtland H-W, Kennedy OD, Wu Y, Gao Y, Sun H, Schaffler MB, et al., Low levels of plasma IGF-1 inhibit intracortical bone remodeling during aging, Age. 35 (2013) 1691–1703. doi:10.1007/s11357-012-9469-8. [PubMed: 22976122]

[32]. Eriksson SA, ISBERG BO, LINDGREN JU, Prediction of vertebral strength by dual photon absorptiometry and quantitative computed tomography, Calcif Tissue Int. 44 (1989) 243–250. doi:10.1007/bf02553758. [PubMed: 2501006]

[33]. Tabensky AD, Williams J, DeLuca V, Briganti E, Seeman E, Bone mass, areal, and volumetric bone density are equally accurate, sensitive, and specific surrogates of the breaking strength of the vertebral body: an in vitro study, J Bone Miner Res. 11 (1996) 1981–1988. doi:10.1002/jbmr.5650111221. [PubMed: 8970902]

[34]. Ito M, Nishida A, Aoyagi K, Uetani M, Hayashi K, Kawase M, Effects of risedronate on trabecular microstructure and biomechanical properties in ovariectomized rat tibia, Osteoporos Int. 16 (2005) 1042–1048. doi:10.1007/s00198-004-1802-3. [PubMed: 15711780]

[35]. Ito M, Nakayama K, Konaka A, Sakata K, Ikeda K, Maruyama T, Effects of a prostaglandin EP4 agonist, ONO-4819, and risedronate on trabecular microstructure and bone strength in mature ovariectomized rats, 39 (2006) 453–459. doi:10.1016/j.bone.2006.02.054.

[36]. Perrien DS, Akel NS, Edwards PK, Carver AA, Bendre MS, Swain FL, et al., Inhibin A is an endocrine stimulator of bone mass and strength, Endocrinology. 148 (2007) 1654–1665. doi:10.1210/en.2006-0848. [PubMed: 17194739]

[37]. Altman AR, Tseng W-J, de Bakker CMJ, Huh BK, Chandra A, Qin L, et al., A closer look at the immediate trabecula response to combined parathyroid hormone and alendronate treatment, Bone. 61 (2014) 149–157. doi:10.1016/j.bone.2014.01.008. [PubMed: 24468717]

[38]. Boyd SK, Szabo E, Ammann P, Increased bone strength is associated with improved bone microarchitecture in intact female rats treated with strontium ranelate: a finite element analysis study, 48 (2011) 1109–1116. doi:10.1016/j.bone.2011.01.004.

[39]. Morrow R, Deyhim F, Patil BS, Stoecker BJ, Feeding orange pulp improved bone quality in a rat model of male osteoporosis, J Med Food. 12 (2009) 298–303. doi:10.1089/jmf.2008.0145. [PubMed: 19459729]

[40]. Alwood JS, Yumoto K, Mojarrab R, Limoli CL, Almeida EAC, Searby ND, et al., Heavy ion irradiation and unloading effects on mouse lumbar vertebral microarchitecture, mechanical properties and tissue stresses, Bone. 47 (2010) 248–255. doi:10.1016/j.bone.2010.05.004. [PubMed: 20466089]

[41]. Wu X, Ding J, Xu X, Wang X, Liu J, Jiang J, et al., Ketogenic diet compromises vertebral microstructure and biomechanical characteristics in mice, J. Bone Miner. Metab 37 (2019) 957–966. doi:10.1007/s00774-019-01002-2. [PubMed: 30968187]

[42]. Shahnazari M, Yao W, Dai W, Wang B, Ionova-Martin SS, Ritchie RO, et al., Higher doses of bisphosphonates further improve bone mass, architecture, and strength but not the tissue material properties in aged rats, Bone. 46 (2010) 1267–1274. doi:10.1016/j.bone.2009.11.019. [PubMed: 19931661]

[43]. Spatz JM, Ellman R, Cloutier AM, Louis L, van Vliet M, Suva LJ, et al., Sclerostin antibody inhibits skeletal deterioration due to reduced mechanical loading, 28 (2013) 865–874. doi:10.1002/jbmr.1807.

[44]. Camargos GV, Bhattacharya P, van Lenthe GH, Del Bel Cury AA, Naert I, Duyck J, et al., Mechanical competence of ovariectomy-induced compromised bone after single or combined treatment with high-frequency loading and bisphosphonates, Sci Rep. 5 (2015) 10795–9. doi:10.1038/srep10795. [PubMed: 26027958]

[45]. Takao-Kawabata R, Isogai Y, Takakura A, Shimazu Y, Sugimoto E, Nakazono O, et al., Three-Times-Weekly Administration of Teriparatide Improves Vertebral and Peripheral Bone Density, Microarchitecture, and Mechanical Properties Without Accelerating Bone Resorption in Ovariectomized Rats, Calcif Tissue Int. (2015) 1–13. doi:10.1007/s00223-015-9998-0.

[46]. Wernle JD, Damron TA, Allen MJ, Mann KA, Local irradiation alters bone morphology and increases bone fragility in a mouse model, J Biomech. 43 (2010) 2738–2746. doi:10.1016/j.jbiomech.2010.06.017. [PubMed: 20655052]

[47]. Nyman JS, Merkel AR, Uppuganti S, Nayak B, Rowland B, Makowski AJ, et al., Combined treatment with a transforming growth factor beta inhibitor (1D11) and bortezomib improves bone architecture in a mouse model of myeloma-induced bone disease, 91 (2016) 1–12. doi:10.1016/j.bone.2016.07.007.

[48]. Creecy A, Uppuganti S, Girard MR, Schlunk SG, Amah C, Granke M, et al., The age-related decrease in material properties of BALB/c mouse long bones involves alterations to the extracellular matrix, Bone. 130 (2020) 115126. doi:10.1016/j.bone.2019.115126. [PubMed: 31678497]

[49]. Lloyd AA, Wang ZX, Donnelly E, Multiscale Contribution of Bone Tissue Material Property Heterogeneity to Trabecular Bone Mechanical Behavior, J Biomech Eng. 137 (2015) 010801. doi:10.1115/1.4029046.

[50]. Zapata E, Follet H, Mitton D, Homogeneous and heterogeneous finite element models to predict radius bone strength in forward fall configuration, Comput Methods Biomech Biomed Engin. 18 Suppl 1 (2015) 2084–2085. doi:10.1080/10255842.2015.1069595. [PubMed: 26259640]

Highlights

- Vertebra strength is lower at 6-months than at 20-months of age in male BALB/c mice.
- Regardless of sex, trabecular bone volume fraction primarily explains strength.
- Micro-finite element analysis predicts failure force but not independently of age.
- Drugs to combat aging effects on spinal fracture risk can be tested in the BALB/c mouse.

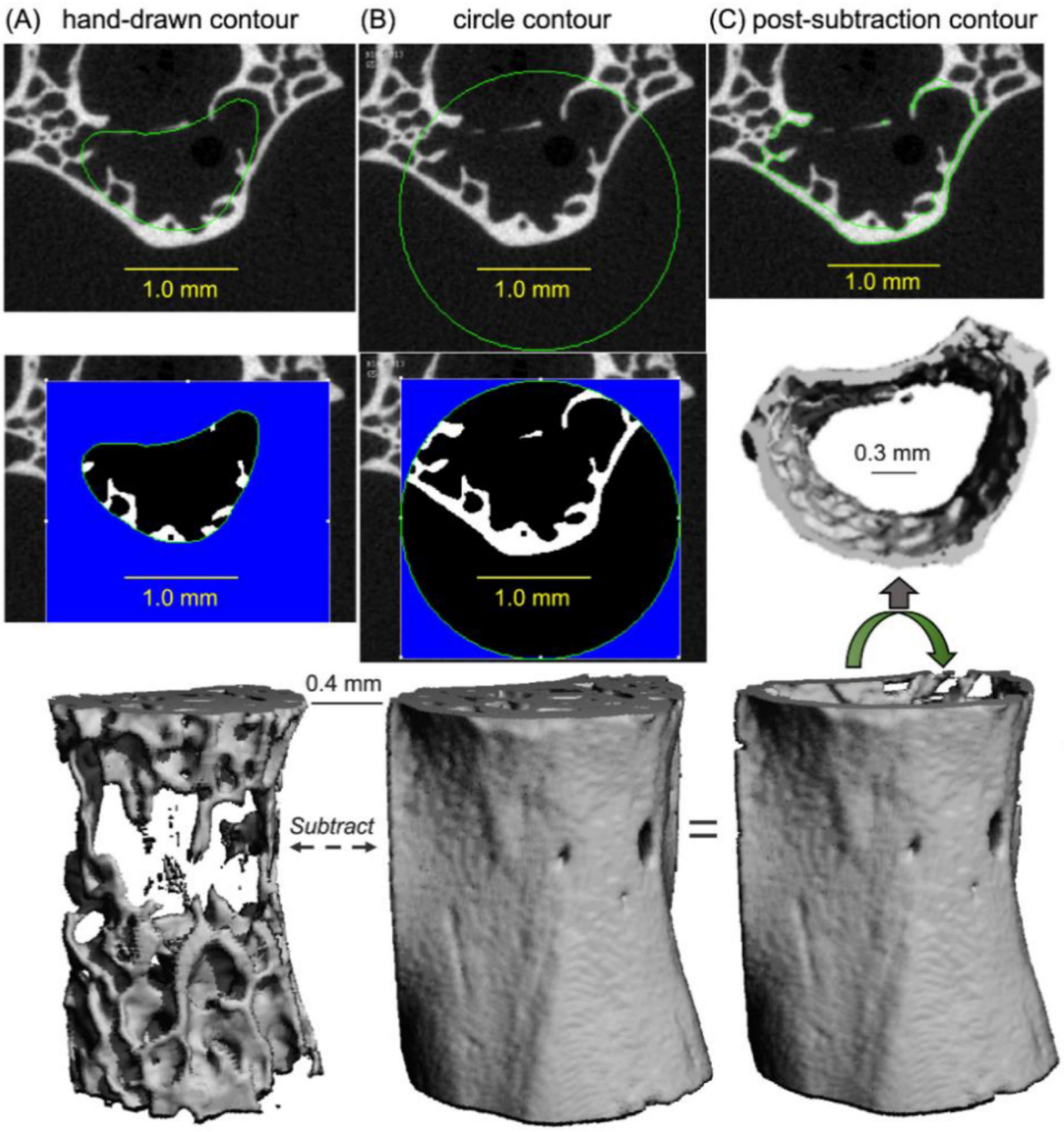

Figure 1.

Contouring procedure to select different regions of interest (L6 VB from a 20-mo. female mouse). Inner contours were drawn by hand to isolate the trabecular bone from the surrounding cortex (A). A circle contour with a constant radius was used to transect the transverse processes, thereby isolating the centrum (B). Upon subtracting the segmented images of trabecular bone from the segmented images of the VB, the cortical shell was isolated for evaluation.

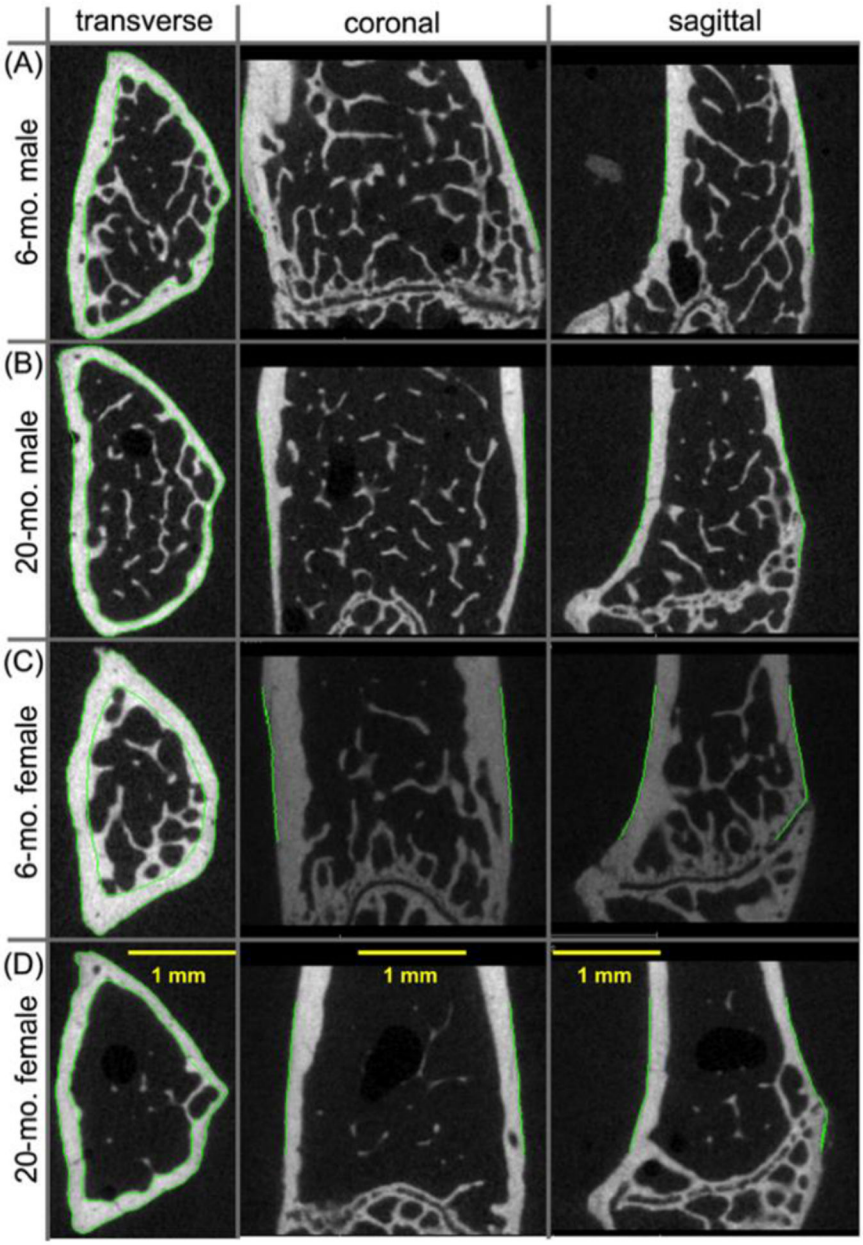

Figure 2.

Two-dimensional μCT images of the distal femur metaphysis from BALB/c mice. The amount of trabecular bone in 6-mo., male mice (A) was higher than the amount of trabecular in 20-mo., male mice (B). Similarly, the amount of trabecular bone appeared to decrease between 6-mo. (C) than at 20-mo. (D) of age in the female mice.

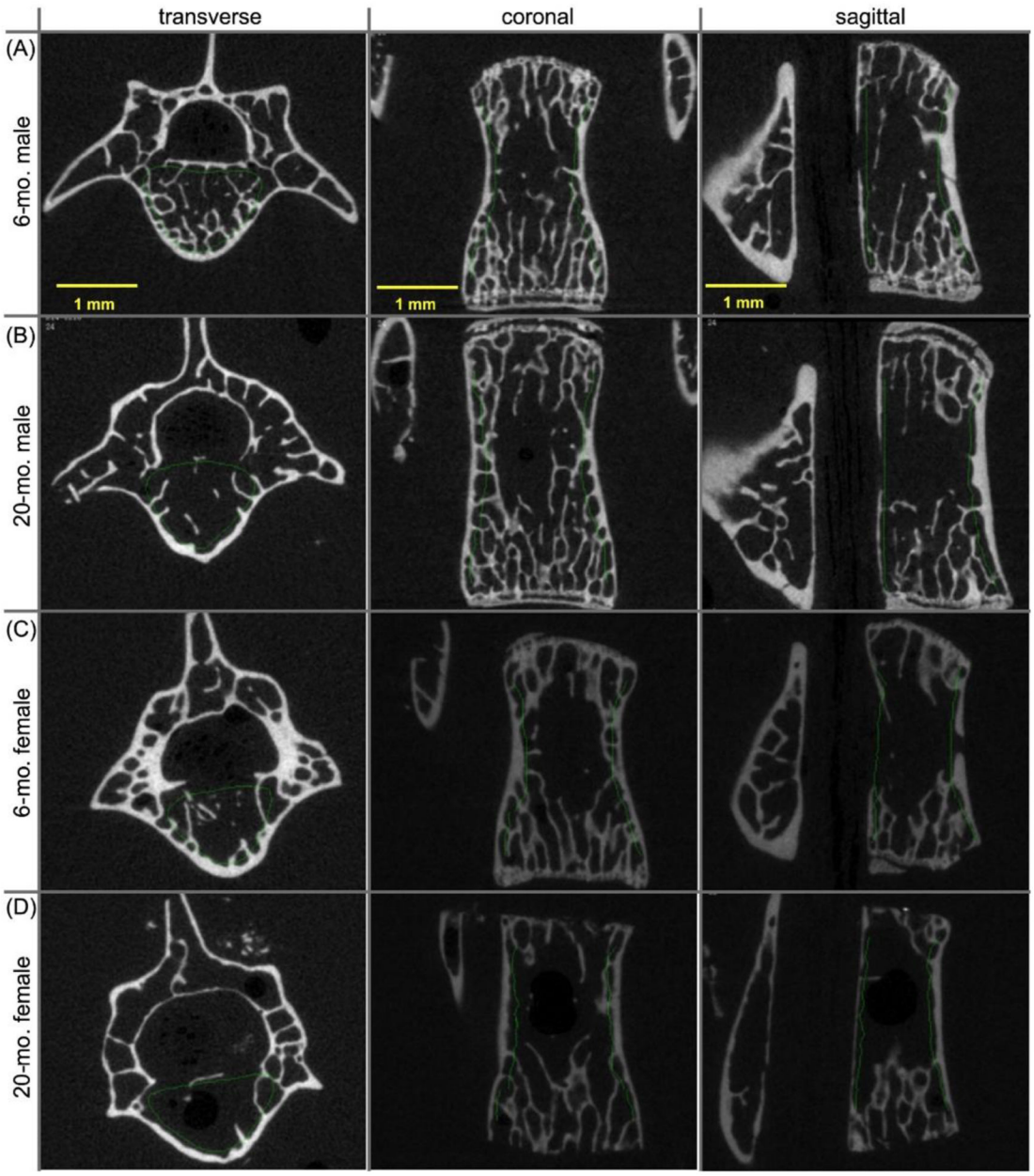

Figure 3.

Two-dimensional μCT images of the L6 vertebral body from BALB/c mice. The amount of trabecular bone in 6-mo. male mice (A) was higher than the amount of trabecular in 20-mo. male mice (B). However, there was not an obvious difference in the amount of trabecular bone between 6-mo. female (C) and 20-mo. female mice (D).

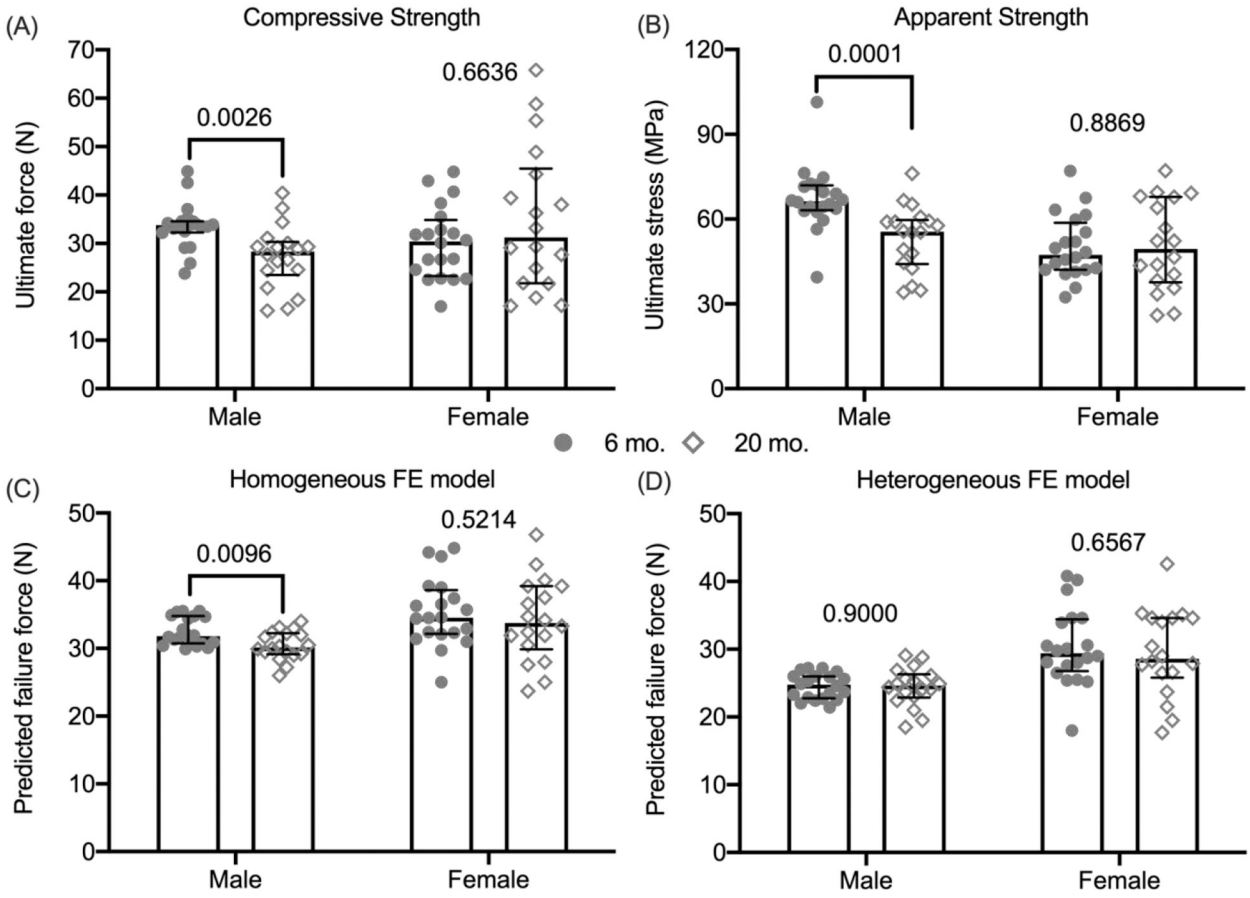

Figure 4:

Compressive strength estimates of the L6 vertebra. The ultimate or maximum force experienced by the L6 VB during compression was significantly lower for the male 20-mo. than for the male 6-mo. old mice (A). After dividing the ultimate force by the cross-sectional bone area of the VB, the ultimate stress was still significantly lower with age in male mice (B). Assuming all bone tissue had the same modulus (18 GPa), μFEA predicted an age-related loss in VB strength for male mice only (C). Assuming the modulus varied among regions based on the distribution of TMD, μFEA predicted that VB strength did not vary with age for both female and male mice (D). P-values for the age comparison are given above the data points with brackets indicating $p<0.05$. median ± interquartile range

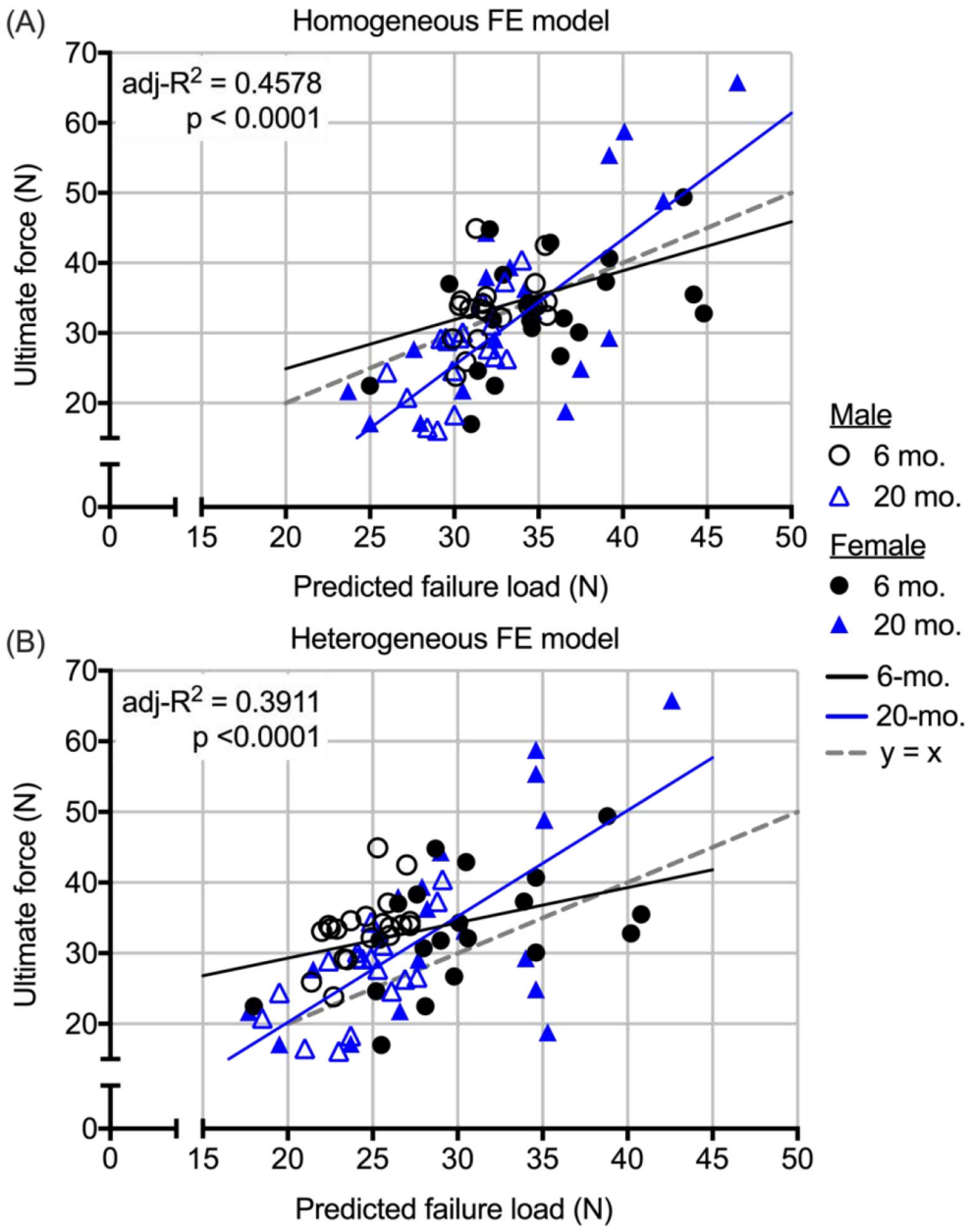

Figure 5.

Multiple linear regressions between the ultimate force from compression tests and predicted failure force from μFEAs. The slope of the line for 20-mo. mice was steeper than the slope of the line for 6-mo. mice, irrespective of whether strength was predicted by homogeneous FE model (A) or an heterogeneous FE model (B). Not only is the adjust coefficient of determination (adj-R^2) higher for the H-μFEA, the data points are more equally distributed above and below the unity line than the data points for I-μFEA.

Table 1:

Age-related differences in the strength of vertebral bodies from published studies involving NIA-supported rodent strains. Percent Difference = 100 × (Old Mean − Young Mean) / Young Mean.

Property	Age comparison	% Difference (% COV[a])	Significant	Reference
Ultimate force of L5 VB	BALB/c	F: −22.2 (15.3 & 31.0)	F: Yes	[18]
	7-mo. vs. 20-mo.	M: −25.6 (32.3 & 21.7)	M: Yes	
Apparent stress[b] of L6 VB	C57BL/6	F: −57[c] (dot plot)	F: Yes	[16]
	8-mo. vs. 25-mo.	M: −40[c] (dot plot)	M: Yes	
Ultimate force of T? VB	C57BL/6J	F: −20 (13 & 17)[d]	F: No	[17]
	6-mo. vs. 18-mo.	M: −14 (20 & 20)[d]	M: No[e]	
Apparent stress[c] of T? VB	C57BL/6J	F: −43 (14 & 33)[d]	F: Yes	[17]
	6-mo. vs. 18-mo.	M: −7 (23 & 17)[d]	M: No	
Ultimate force of L6 VB	F344BN rats	Male only		[19]
	8-mo. vs. 28-mo.	M: 1.2 (23.3 & 29.6)	M: No	
	8-mo. vs. 36-mo.	M: 15.3 (23.3 & 14.0)	M: No	
Ultimate force of L5 VB	F344 rats	Male only		[12]
	6-mo. vs. 12-mo.	M: 10.2 (422.6 & 985.6)	M: No	
	6-mo. vs. 24-mo.	M: −6.3 (422.6 & 303.3)	M: No	
	12-mo. vs. 24-mo.	M: −14.9 (985.6 & 303.3)	M: No	

[a] Coefficient of variance = 100 × Mean / SD for young & old rodents, respectively

[b] Ultimate force divided by cross-sectional area assuming the area was elliptical.

[c] Ultimate force divided by cross-sectional area assuming the area was circular.

[d] Estimated from bar graphs

[e] Significant in two-way ANOVA in which age and diet (low AGE and high AGE) were the main effects but not significant in the post-hoc, pairwise comparisons.

Table 2:

Differences in selected μCT properties of the distal femur between age groups for female and male BALB/c mice.

		Female			Male		
Property[a]	**Unit**	**6-mo. (n=20)**	**20-mo. (n=18)**	**p-value**	**6-mo. (n=20)**	**20-mo. (n=18)**	**p-value**
			Metaphysis (inner trabecular)				
BV/TV	%	11.5 (5.4)	4.5 (4.3)	<0.0001	12.4 (2.6)	9.9 (1.8)	0.0016
Tb.N	Mm^{-1}	3.06 (0.57)	1.91 (0.49)	<0.0001	4.56 (0.43)	4.18 (0.59)	0.0355
Tb.Th	μm	52.6 (5.2)	53.8 (7.7)	0.5605	43.6 (4.6)	40.4 (5.0)	0.0052
Tb.Sp	μm	340 (65)	568 (178)	<0.0001	220 (23)	241 (38.0)	0.0832
Conn.D	mm^{-3}	48 (22)	10 (14)	<0.0001	137 (42)	93 (37)	0.0015
SMI	1=plate 3=rod	1.68 (0.53)	2.57 (0.81)	0.0004	2.04 (0.31)	2.08 (0.24)	0.6494
Tb.avBMD	$mgHA/cm^3$	190 (62)	96 (51)	<0.0001	200 (28)	177 (22)	0.0079
Tb.TMD	$mgHA/cm^3$	1009 (25)	1064 (28)	<0.0001	1000 (20)	1032 (18)	<0.0001
			Metaphysis (outer cortex)				
Met.Tt.Ar	mm^2	1.01 (0.15)	1.00 (0.19)	0.9167	0.929 (0.11)	0.786 (0.14)	0.0018
Met.Th	μm	0.135 (0.016)	0.121 (0.018)	0.1180	0.109 (0.012)	0.098 (0.008)	0.0146
Met.Po	%	7.25 (2.08)	9.26 (4.85)	0.3805	9.29 (1.78)	7.68 (2.05)	0.0146
Met.TMD	$mgHA/cm^3$	1206 (23)	1246 (31)	<0.0001	1156 (19)	1178 (14)	0.0002

[a]Mean (SD)

Table 3.

Differences in selected μCT-derived properties of L6 VB between age groups

		Female			Male		
Property[a]	**Unit**	**6-mo. (n=20)**	**20-mo. (n=18)**	**p-value**	**6-mo. (n=20)**	**20-mo. (n=18)**	**p-value**
			Centrum (inner)				
BV/TV	%	23.1 (4.4)	22.7 (7.6)	0.8135	23.0 (1.7)	20.1 (1.5)	<0.0001
Tb.N	mm^{-1}	3.51 (0.47)	3.01 (0.70)	0.0149	5.20 (0.21)	4.87 (0.24)	<0.0001
Tb.Th	μm	54.7 (4.00)	57.2 (13.0)	0.1232	46.0 (2.00)	43.0 (2.00)	0.0001
Tb.Sp	μm	303 (43.0)	365 (82.0)	0.0354	194 (9.00)	206 (11.0)	0.0006
Conn.D	mm^{-3}	82.7 (14.0)	60.5(36.7)	0.0005	306 (32.5)	256 (41.7)	0.0003
Tb.vBMD	$mgHA/cm^3$	278 (51)	271 (85)	0.7655	295 (17)	267 (18)	<0.0001
Tb.TMD	$mgHA/cm^3$	1014 (33)	1028 (27)	0.1697	1000 (15)	1019 (20)	0.0030
			Cortex (shell)				
Sh.Ar	mm^2	0.391 (0.061)	0.387 (0.057)	0.8426	0.318 (0.051)	0.261 (0.091)	0.0254
Sh.Th	μm	0.080 (0.007)	0.074 (0.009)	0.0207	0.067 (0.009)	0.066 (0.007)	0.8015
Sh.TMD	$mgHA/cm^3$	1096 (18)	1108 (18)	0.0475	1063 (14)	1096 (18)	<0.0001
			Body without TPs (circle)				
B.Ar	mm^2	0.666 (0.102)	0.679 (0.133)	0.7397	0.613 (0.039)	0.602 (0.049)	0.4670
Ax.Le	mm	2.05 (0.30)	2.26 (0.43)	0.0964	2.87 (0.17)	3.04 (0.09)	0.0006
Tt.TMD	$mgHA/cm^3$	1074 (19)	1082 (18)	0.2138	1053 (10)	1080 (14)	<0.0001

[a]Mean (SD)

Table 4.

Correlations between the ultimate compressive force of L6 VBs and potential explanatory variables as given by either Spearman r (*p-value*) or Pearson r (*p-value*).

Variable	Female[a] N=38	Female 6-mo.[a] N=20	Female 20-mo.[a] N=18	Male[b] N=38	Male 6-mo.[a,b] N=20	Male 20-mo.[b] N=18
Heterog-μFEA	0.5314 *(0.0006)*	N/A[c]	N/A	N/R[d]	0.5381 *(0.0144)*[b]	0.6579 *(0.0030)*
Homog-μFEA	0.5447[e] *(0.0004)*	0.4077 *(0.0744)*	0.6880 *(0.0016)*	0.6377 *(<0.0001)*	0.3794 *(0.0990)*[a]	0.6528 *(0.0033)*
BV/TV	0.6211 *(<0.0001)*	N/A	N/A	0.5214 *(0.0008)*	N/A	N/A
Tb.vBMD	0.6000 *(<0.0001)*	N/A	N/A	0.4883 *(0.0019)*	N/A	N/A
Tb.N	0.4335 *(0.0066)*	N/A	N/A	N/R	– *(0.8965)*[b]	– *(0.7358)*
Conn.D	– *(0.0862)*	N/A	N/A	N/R	– *(0.4939)*[b]	– *(0.2022)*
Sh.Th	– *(0.2771)*	N/A	N/A	N/R	*(0.5438)*[b]	0.435 *(0.003)*
B.Ar	0.5291 *(0.0006)*	N/A	N/A	N/R	– *(0.3065)*[a]	0.6612 *(0.0028)*
Ax.Le	– *(0.2447)*	N/A	N/A	N/R	0.5102 *(0.0275)*[b]	– *(0.1186)*
Tt.TMD	– *(0.6203)*	N/A	N/A	N/R	– *(0.0853)*[b]	– *(0.4112)*

[a] Spearman correlation because the residuals of most regressions for the female data did not pass normality or homoscedasticity tests

[b] Pearson correlation because the residuals of nearly all regressions passed normality or homoscedasticity test (2 exceptions in which case Spearman's correlation was used)

[c] Not applicable (N/A) because one straight line most likely explains all the data

[d] Not relevant (N/R) because 2 different straight lines likely explain the data, one for each age group

[e] The probability that one straight line explains all the data is nearly equivalent to the probability that 2 different straight lines explain the data, one for each age group

Table 5.

Coefficients (and their p-value) for multiple linear regressions between explanatory variable(s) and the ultimate compressive force of L6 VBs with and without 2 categorical covariates (Cvar) including interactions (p<0.06). N=76 mice

Explanatory variables	Model:	Reference[a]		Coefficient 1[b]		Coefficient 2[c]		Cvar[d]	Inter[e]	Adj-R^2
H-μFEA+Age	**6-mo.:**	**+10.9**	(p=0.261)	**+0.7**	**(*p=0.018*)**	–	–	**(*p=0.005*)**	**(*P=0.007*)**	**0.4578**
	20-mo.:	**−28.6**		**+1.8**						
I-μEA+Age	6-mo.:	+19.3	(*p=0.001*)	+0.5	(*p=0.018*)	–	–	(*P=0.005*)	(*P=0.015*)	0.3911
	20-mo.:	−9.8		+1.5						
BV/TV [g]	**All:**	**+2.5**	(p=0.656)	**+133.7**	**(*p<0.0001*)**	–	–	**NI**	**NI**	**0.4067**
Tb.vBMD+Sex	F:	+2.1	(p=0.707)	+0.1	(*p<0.0001*)	–	–	(*P=0.023*)	NI	0.3972
	M:	−2.0								
Tb.N+Age+Sex[f]	F/6-mo.:	+0.64		+9.26				(p=0.074)	(*P=0.026*)	0.1976
	F/20-mo.:	+7.04								
	M/6-mo.:	+41.83		−1.59						
	M/20-mo.:	+35.03	(*p=0.007*)							
B.Ar+Age	6-mo.:	+11.9	(p=0.195)	+33.5	(*P = 0.016*)	–	–	(*P=0.017*)	(*P=0.030*)	0.4062
	20-mo.:	−20.2		+80.0						
Sh. Th	All:	+13.9	(p=0.128)	+255.3	(*p=0.048*)	–	–	NI	NI	0.0559
Tb.vBMD+B.Ar	**All:**	**−8.0**	(p=0.267)	**+0.064**	**(*p=0.015*)**	**+35.0**	**(*p=0.028*)**	**NI**	**NI**	**0.3985**

[a] As the intercept term in the GLM, the reference value is always included even if it is not significant. There are 2 reference values when one of the covariates is in included in the regression model.

[b] Coefficient 1 belongs to the first explanatory variable in the model (first column). There are 2 values when the variable interacts with one of the covariates.

[c] Coefficient 2 belongs to the second explanatory variable if included in the model. There are 2 values when the variable interacts with one of the covariates.

[d] Sex or age group is the second or third explanatory variable depending on the model. In some regressions, it was not included (NI) in the GLM because it was removed due to a lack of significance.

[e] An interaction term was included in the model when significant. Otherwise, it was removed.

[f] There is a significant interaction between sex and age of the animal as well as between sex and Tb.N.

[g] Tb.N, B.Ar, and Sh.Th do not help BV/TV explain the variance in VB strength (ultimate force).